https://doi.org/10.22226/2410-3535-2021-4-427-432 PACS: 81.20.-n; 62.20.-x

Microstructure and mechanical properties of low-carbon steel fabricated by electron-beam additive manufacturing

E. G. Astafurova†, E. V. Melnikov, S. V. Astafurov, M. Yu. Panchenko, K. A. Reunova, V. A. Moskvina, G. G. Maier, E. A. Kolubaev

†elena.g.astafurova@ispms.ru

Institute of Strength Physics and Materials Science SB RAS, Tomsk, 634055, Russia

The microstructure and mechanical properties of a billet obtained by electron-beam additive manufacturing (EBAM) using an industrial welding wire of low-carbon steel were studied. After EBAM, the steel billet possesses the phase composition constant in volume (ferrite with carbides). Deformation behavior of samples of steel obtained by the additive methods depends on their position in the billet. In its lower part, which is characterized by a high cooling rate in the EBAM-process, predominantly equiaxed ferrite grains with an average size of 15 μm are formed. The mechanical properties and deformation behavior (the presence of a yield plateau, the stages of plastic flow) of this part of the billet are close to those of normalized low-carbon steel obtained by conventional methods of metallurgy and thermomechanical processing. In the middle and top parts of the billet, the coarse non-equiaxed ferritic grains (hundreds of micrometers) form. The mechanical properties in this part weakly depend on the position of the samples and their orientation relative to the building direction of the billet — the yield plateau disappears; the yield stress, the ultimate tensile strength, the elongation become lower than those of the normalized low-carbon steel obtained by the conventional method. Despite the predominance of ferritic grains (with carbides), a small portion of grains with a lamellar ferrite morphology resembling martensite or bainite is observed in all parts of the billet. The latter is the result of a complex thermal history of the billet, which can undergo multiple phase transformations during successive heating and cooling cycles.

Keywords: low-carbon steel, electron-beam additive manufacture, mechanical properties, microstructure.

УДК: 672.1; 539.3; 539.4; 538.91

Микроструктура и механические свойства малоуглеродистой стали, полученной методом электронно-лучевого аддитивного производства

Астафурова Е. Г.†, Мельников Е. В., Астафуров С. В., Панченко М. Ю., Реунова К. А., Москвина В. А., Майер Г. Г., Колубаев Е. А.

Институт физики прочности и материаловедения СО РАН, Томск, 634055, Россия

В настоящей работе изучена микроструктура, фазовый состав и механические свойства заготовки из малоуглеродистой стали, полученной методом электронно-лучевого аддитивного производства (ЭЛАП) с использованием промышленной сварочной проволоки марки 08Г2С. Экспериментально показано, что процесс ЭЛАП позволяет сформировать стальную заготовку малоуглеродистой стали с постоянным по объему фазовым составом (феррит с карбидами). При этом деформационное поведение аддитивно-полученной стали зависит от положения образцов в заготовке. В нижней ее части, для которой характерна высокая скорость охлаждения в процессе ЭЛАП, происходит формирование преимущественно равноосных ферритных зерен со средним размером 15 мкм. Механические свойства и деформационное поведение (наличие площадки текучести, стадийность пластического течения) этой части заготовки близки к свойствам нормализованной стали 09Г2С, полученной традиционными методами металлургии и термомеханической обработки. В остальной части заготовки (центральной и верхней) формируется структура с неравноосными ферритными зернами, размеры которых достигают сотен микрометров. Механические

свойства в этой части слабо зависят от положения образцов и их ориентации относительно направления роста заготовки — площадка текучести вырождается, пределы текучести и прочности, удлинения становятся ниже, чем у нормализованной стали 09Г2С, полученной традиционным способом. Несмотря на преобладание ферритных зерен (с карбидами), во всех частях заготовки наблюдается небольшая доля зерен с пластинчатой морфологией феррита, напоминающей мартенсит или бейнит. Последнее является результатом сложной термической истории заготовки, которая в процессе последовательных циклов нагрева и охлаждения может претерпевать многократные фазовые превращения.

Ключевые слова: малоуглеродистая сталь, электронно-лучевое аддитивное производство, механические свойства, микроструктура.

1. Introduction

The development of additive manufacturing is focused on obtaining new promising materials or adapting the technological cycle to produce conventional alloys. Low-carbon steels are among the most demanded structural materials in the world. They combine low cost and excellent mechanical properties, which can be varied over a wide range [1]. Additive technologies, including electron-beam additive manufacturing (EBAM), allow forming large-scale products of various shapes and complex internal architecture [2, 3]. Despite the perspective of additive manufacture of steel [4], there are still not so many works exploring additively-produced low-carbon steels [5 – 7]. Ahsan et al. [5] studied the structure and mechanical properties of low-carbon steel, produced by wire arc additive manufacturing (WAAM). They showed that steel possesses a mixed structure with acicular, polygonal and Widmanstatten ferrite, while they did not reveal any segregations or heterogeneity in the elemental composition. Under tension such steel demonstrates rather low mechanical properties: the yield stress less than 300 MPa and the elongation ≈10%. The authors of the research [6] also used the WAAM method to form a billet from low-carbon steel. But its mechanical properties were high: yield stress approximately equal to 800 MPa and elongation 10 –12%, the authors revealed anisotropy of mechanical properties in the additively-obtained specimens. The structure was heterogeneous throughout the billet and consisted of a mixture of ferrite, troostite, and austenitic-martensitic areas. The authors of [7], on the contrary, noted the absence of anisotropy of mechanical properties in low-carbon steel produced by submerged arc additive manufacturing. They suggested that due to multiple heating and cooling cycles of the billet under additive manufacturing, elongated large ferrite grains undergo multiple allotropic transformations and recrystallize with the formation of fine-grained ferrite (yield stress is 330 – 346 MPa, elongation 32 – 39%).

In view of the complex thermal history and, as a consequence, the variety of the resulting phase compositions, detailed studies on the effect of additive manufacturing methods and regimes on the properties of such steels are required. In this work, we studied the microstructure, phase composition and mechanical properties in different parts of a steel billet obtained by the EBAM method using a low-carbon steel wire.

2. Materials and methods

Using a laboratory unit for EBAM, a steel billet (wall) with linear dimensions of 110 × 30 × 5 mm was produced. A welding wire Fe-(1.8 – 2.1)Mn-(0.7 – 0.95)Si-(0.05 – 0.11)C (mass.%) with a diameter of 1.2 mm was used as the raw material. The following technological parameters were used: beam current 44 – 50 mA, accelerating voltage 30 kV, wire feeding rate 350 mm/min, ellipse-shaped beam of 3 × 4 mm and scanning frequency 1 kHz. The process was conducted in vacuum ($P = 1 \times 10^{-3}$ Pa). The wall was obtained by sequential layer-by-layer deposition of 30 parallel layers (Fig. 1a). The substrate material (austenitic stainless steel) was not cooled during EBAM.

Flat proportional dumbbell-shaped specimens were cut from the resulting billet. A scheme of the orientation of tensile specimens in the billet is shown in Fig. 1b. After mechanical grinding and electrolytic polishing in a solution of 25 g CrO_3 + 200 ml H_3PO_4, the dimensions of the gauge sections of the specimens were 12 × 2.6 × 1.2 mm.

To compare the mechanical properties of additively-manufactured low-carbon steel (AM-LCS) with that obtained by conventional methods (C-LCS), specimens of industrial low-carbon steel (Fe-(1.3 –1.7)Mn-(0.5 – 0.8)Si-<0.12 C, mass.%) were prepared. They were subjected to normalization at a temperature of 980°C for 0.5 h with air cooling.

Mechanical tests of the specimens were conducted by the method of uniaxial static tension at room temperature and an initial strain rate of 5×10^{-4} s^{-1} using an LFM-125 testing machine (Walter+Bai AG).

X-ray diffraction (XRD) phase and structural analyses were carried out using a DRON 7 diffractometer (Bourevestnik) with Co-Kα radiation. The crystal lattice parameters of the ferrite phase (a) were calculated by extrapolation the dependence of the a_{hkl}-values, obtained for each X-ray line with the (hkl) indices, plotted against the ($\cos\theta \cot\theta$) function. Analysis of the microstructure of the specimens was performed using a scanning electron microscope (SEM, LEO EVO 50, Zeiss). In addition to the SE-SEM (secondary electrons) regime, the BSE-SEM (back scattered diffraction) regime was used. Before structural studies, the surface of the specimens was chemically etched in a solution of 50 ml H_2O + 5 g $FeCl_3$. Flat specimens for microstructural analysis were cut normal to the deposition direction.

3. Results and discussion

Figs. 1c and 2 show XRD patterns and SEM images for steel specimens obtained by different methods.

All XRD patterns contain reflections corresponding α-Fe with a bcc crystal lattice. The microstructure of C-LCS steel was a ferritic-pearlitic mixture with a ferrite lattice parameter $a = 2.8699 \pm 0.0013$ Å. The average size of ferritic grains is $d_f = 17 \pm 3$ μm. The microstructure of ferritic-pearlitic steel is

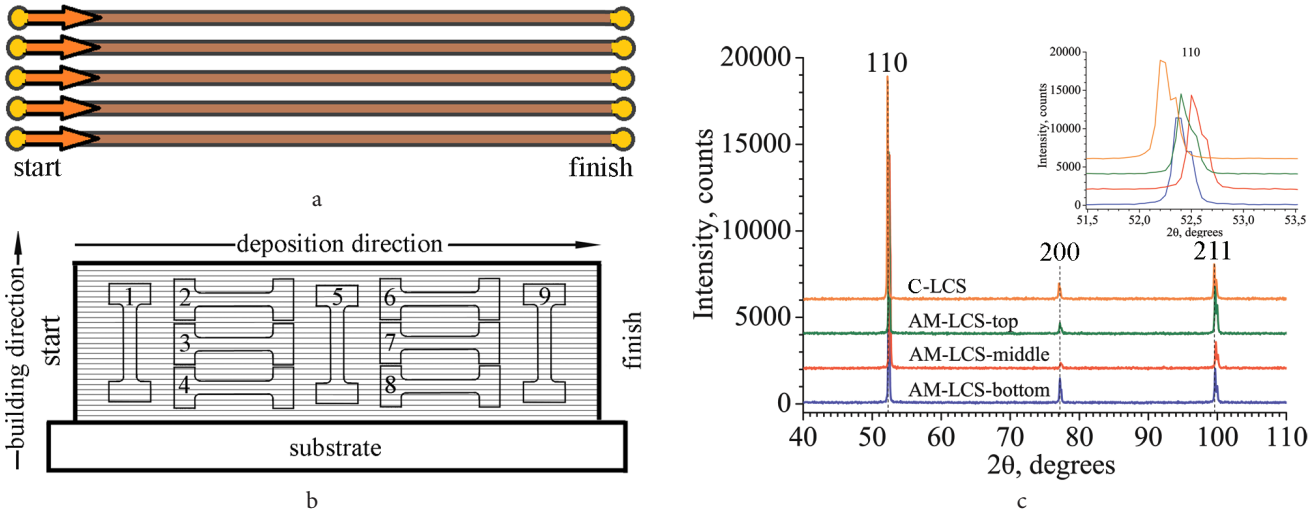

Fig. 1. (Color online) Scheme of deposition in EBAM (a), scheme of orientation of tensile specimens relative to the building direction (b), XRD patterns for C-LCS and AM-LCS (for different parts of the wall) (c).

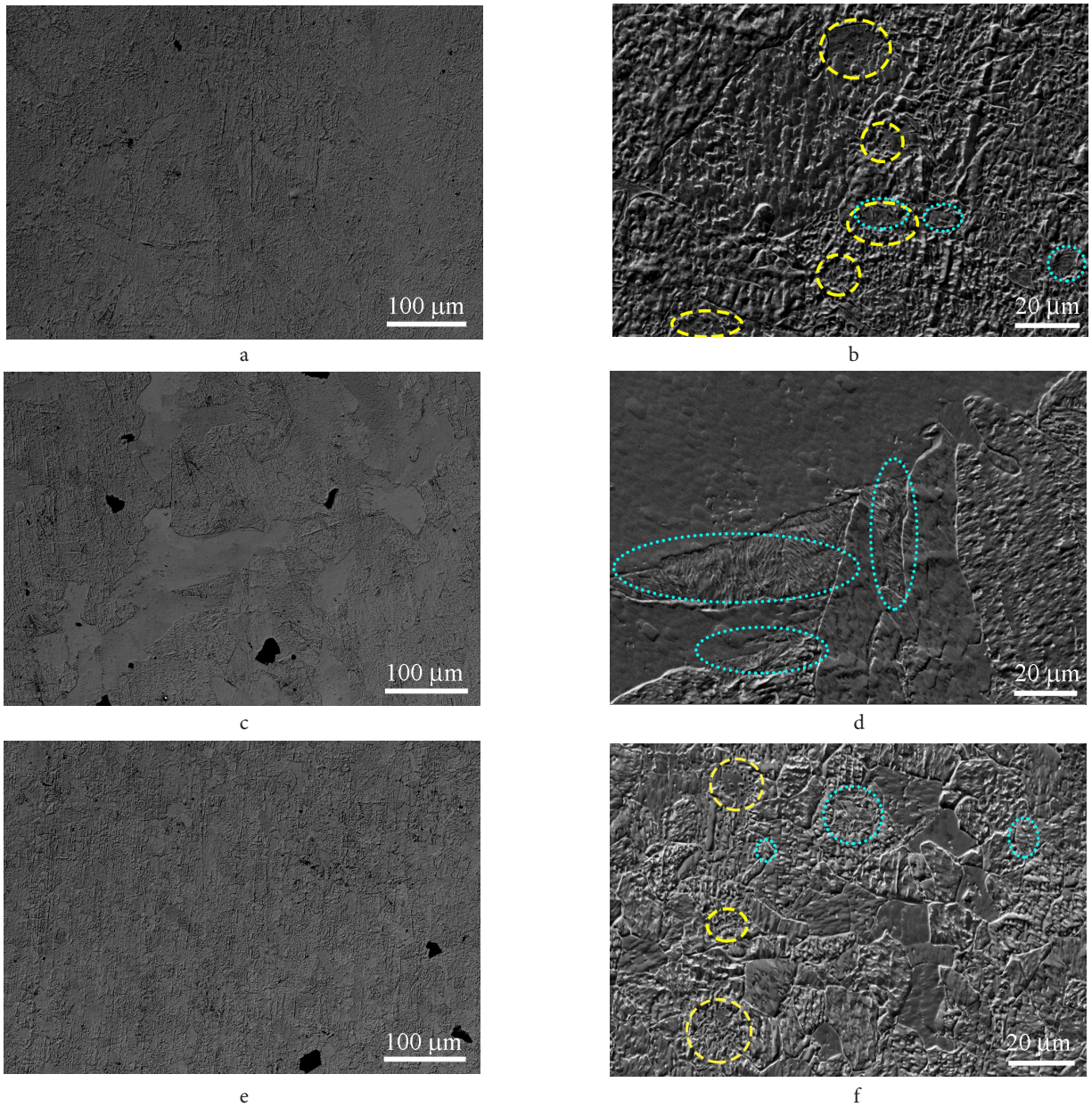

Fig. 2. (Color online) SEM-images of the microstructure of AM-LCS specimens: top (a, b), middle (c, d), and bottom (e, f) parts of the wall (at the distance of 5, 15 and 25 mm to the substrate). BSE-SEM regime (a, c, e); SE-SEM regime (b, d, f).

similar to that previously described in [1,8]. The XRD results showed that the lattice parameter of AM-LCS additive steel weakly depends on the specimen position in the billet: in the lower part ("bottom") it is 2.8693 ± 0.0010 Å, in the central ("middle") — 2.8695 ± 0.0015 Å, in the upper ("top") — 2.8698 ± 0.0016 Å. These values are close to the data for C-LCS steel in the normalized state. Despite this, a shift of $(110)_\alpha$ X-ray lines is observed in the additively-manufactured specimens relative to C-LCS ones (Fig. 1c, insert), which could be associated both with the internal stresses inherent in additive materials and with a possible phase transformation during heating-cooling cycles [9].

The microstructure of the additively-manufactured specimens is heterogeneous along the wall height (Fig. 2). The main phase is ferrite. Quasi-equiaxial ferritic grains are characteristic of the lower part (Fig. 2e,f), their average diameter is d_f=15 ± 3 μm. In the central and upper parts of the wall, the structure has non-equiaxed coarse ferrite grains, the size of which reaches hundreds of micrometers. The heterogeneous surface relief observed in SEM images is due to the presence of large spherical carbides in the grain bodies, their size reaches 2 μm (grains with large carbides, in which particles are most clearly visible, are highlighted by yellow circles in Fig. 2b,d,f). Spherical grains with lamellar morphology characteristic of the martensite or carbide-free bainite structure [1] is rarely observed (highlighted by blue circles in Fig. 2b,d,f). In the central part of the billet, such lamellar regions are observed more frequently than in the upper and lower parts, they were located at the boundaries of large ferrite grains and their size reached d_m = 50 ± 20 μm (Fig. 2d) (≈10 μm in other parts of the billet). The specimens are completely free of pores. Black areas in Figs. 2a,c, and e arises due to the etching of the specimen and high contrast in the BSE-SEM regime.

The rather fine-grained structure in the lower part of the billet is caused by the high cooling rate at the very beginning of the EBAM process, as was previously shown in [7,10,11]. During the further process, a decrease in the cooling rate is accompanied by grain growth, but the phase transformations occurring in this case prevent the formation of columnar ferrite grains by analogy with the previously established regularities [7]. That is, in contrast to additively-manufactured austenitic steels [10], low-carbon steel is not characterized by the formation of large columnar grains with the length comparable to the wall height.

The cooling rate at the beginning of the process, when the substrate is not yet heated, is probably sufficient for the formation of martensite in the lower part of the billet. But in the process of deposition of subsequent layers, all layers are significantly heated for many times, and the cooling rate

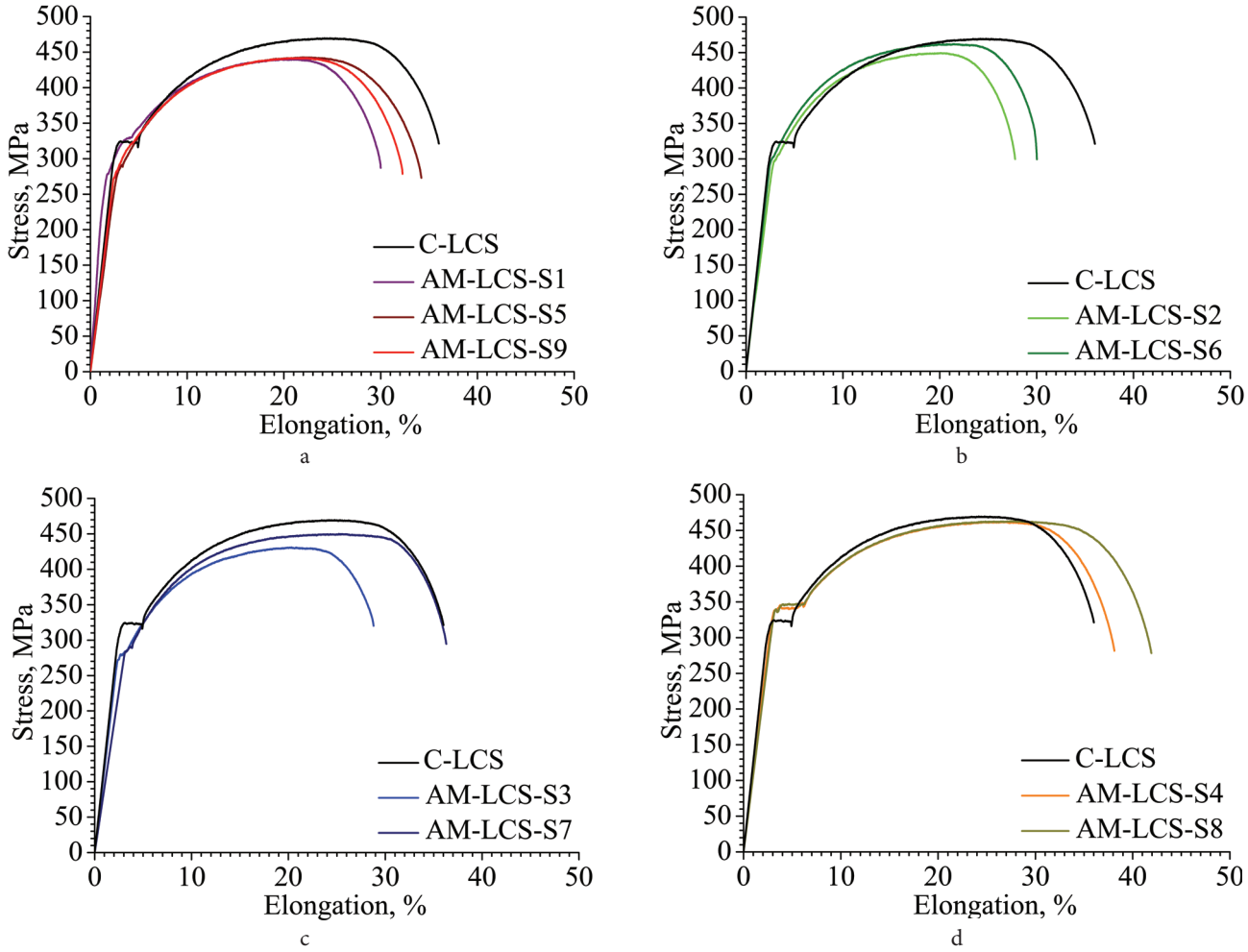

Fig. 3. (Color online) Flow curves in engineering coordinates for samples of C-LCS steel and AM-LCS. The EBAM numbering of samples (1–9) corresponds to the scheme in Fig. 1b.

constantly decreases. That is, with repeated "heating-cooling" cycles, martensite can transform into ferrite of various morphologies or bainite. The ferrite morphology in various parts of the wall is different because of the different rate of crystallization and subsequent "thermal history" (i. e., what was the sequence of phase transformations in "heating-cooling" cycles). Despite the fact that the "thermal history" of various parts of the wall is different, its phase composition is constant (ferrite with carbides), and the main differences are observed, first of all, in the size and shape of ferrite grains.

Fig. 3 shows tensile diagrams for specimens of normalized conventional steel and EBAM-obtained one, depending on the specimens' orientation relative to the building direction of the wall (Fig. 1b). Data on the mechanical properties of the specimens (yield stress ($\sigma_{0.2}$), ultimate tensile strength ($\sigma_{в}$), elongation to failure (δ)) are summarized in Table 1.

The diagrams for C-LCS steel have the form typical for normalized low-carbon steels — with a yield plateau and subsequent parabolic hardening (Fig. 3). Mechanical properties and regularities of plastic flow for additively-manufactured specimens cut in the lower part of the billet (along the direction of deposition layers) are similar to those established for low-carbon conventional steel (Fig. 3 d). These specimens are characterized by a structure with rather fine spherical grains, the size of which (15 μm) is close to the average grain size in C-LCS (17 μm). Despite the close structural parameters and regularities of plastic deformation, the yield stress of the additively-obtained specimens is 10% higher than that of C-LCS (Table 1). The yield plateau, which is typically associated with the formation of the Luders-Chernov band and described by the locking (and unlocking) of dislocations by atmospheres of carbon atoms [12], is also slightly longer in the AM-LCS specimens (Fig. 3 d). All this confirms the assumption that the high rate of cooling of billet at the beginning of the EBAM process provides not only the formation of a fine ferrite grain, but also the preservation of some carbon atoms in the solid solution.

For specimens corresponding to the central and upper parts of the EBAM-manufactured billet, the mechanical properties are close (Table 1). The tensile diagrams of these specimens are similar, but as the upper part of the billet is approached, the length of the yield plateau decreases (Fig. 3 b, c). At the same time, the yield stress values of additively-manufactured specimens are lower than those of normalized steel. A slight anisotropy of mechanical properties is observed (Table 1, Fig. 3 a, b, c). This behavior is due to the formation of large ferritic grains (an order of magnitude larger compared to C-LCS steel) and is in accordance with the data in [5, 7]. A lower crystallization rate and a higher temperature, to which the billet cools down in "heating-cooling" cycles when depositing subsequent layers, promotes grain growth, the formation of carbides and their growth, and the depletion of the solid-solution by interstitial atoms (carbon). Despite the established differences, the mechanical properties of additively-manufactured specimens are not significantly lower than ones of conventional steel, that is, the additively-manufactured constructions can be used without post-production thermal and thermomechanical treatments.

4. Conclusion

A low-carbon steel billet with a constant phase composition (ferrite with carbides) was formed using EBAM. In the lower part of the billet, predominantly equiaxed grains with an average size of 15 μm are formed. In the central and upper parts, a structure with non-equiaxed ferrite grains hundreds of micrometers in size is formed. Despite the predominance of ferritic grains with carbides, a small proportion of grains with a lamellar morphology reminding martensite or bainite is observed in all parts of the billet due to the phase transformations during multiple heating-cooling cycles in the EBAM process.

The mechanical properties of specimens cut from the different parts of the billet are close to those of conventional low-carbon steel with a ferritic-pearlitic structure. The difference in the grain size of ferrite and the morphology of the microstructure influence the deformation behavior of the specimens, but the mechanical properties of the additively-manufactured specimens are not significantly lower than those in conventional steel, that is, the additively-manufactured constructions can be used without post-production thermal and thermomechanical treatments.

Acknowledgements. The work was performed according to the Government research assignment for ISPMS SB RAS, project FWRW-2019-0030. The studies were conducted using the equipment of "Nanotech" center (ISPMS SB RAS, Tomsk).

Table 1. Mechanical properties (yield stress — YS, ultimate tensile strength — UTS, relative elongation — El.) of C-LCS and AM-LCS specimens. The EBAM numbering of samples (1–9) corresponds to the scheme in Fig. 1b.

Notation	YS, MPa	UTS, MPa	El. %
C-LCS	309.6	464.8	35.7
AM-LCS, S1	265.1	439.9	28.5
AM-LCS, S2 (horizontal, start, top)	296.7	449.5	24.9
AM-LCS, S3 (horizontal, start, middle)	273.5	430.1	26.1
AM-LCS, S4 (horizontal, start, bottom)	339.2	461.9	35.6
AM-LCS, S5 (vertical, middle)	280.2	442.7	31.5
AM-LCS, S6 (horizontal, finish, top)	287.3	462.1	27.5
AM-LCS, S7 (horizontal, finish, middle)	284.3	449.8	33.1
AM-LCS, S8 (horizontal, finish, bottom)	339.5	464.7	36.7
AM-LCS, S9 (vertical, finish)	277.1	441.6	29.8

References

1. H. Bhadeshia, R. Honeykombe. Steels: Microstructure and Properties. Elsevier, Amsterdam (2006) 344 p. Crossref
2. W.E. Frazier. J. Mater. Eng. Perform. 23, 1917 (2014). Crossref
3. D. Ding, Z. Pan, D. Cuiuri, H.Li. Int. J.Adv. Manuf. Technol. 81, 465 (2015). Crossref
4. P. Bajaj, A. Hariharan, A. Kini, P. Kurnsteiner, D. Raabe, E.A. Jagle. Mater. Sci. Eng., A. 772, 138633 (2020). Crossref
5. Md.R. U. Ahsan, A.N. M. Tanvir, G.-J. Seo, B. Bates, W. Hawkins, C. Lee, P.K. Liaw, M. Noakes, A. Nycz, D.B. Kim. Additive Manuf. 32, 101036 (2020). Crossref
6. L. Sun, F. Jiang, R. Huang, D. Yuan, C. Guo, J. Wang. Mater. Sci. Eng. A. 787, 139514 (2020). Crossref
7. Y. Li, S. Wu, H. Li, F. Cheng. Mater. Lett. 283, 128780 (2021). Crossref
8. E.D. Merson, P.N. Myagkikh, G.V. Klevtsov, D.L. Merson, A.Y. Vinogradov. Lett. Mater. 10 (2), 152 (2020). Crossref
9. S.Y. Tarasov, A.V. Filippov, N.L. Savchenko, S.V. Fortuna, V.E. Rubtsov, E.A. Kolubaev, S.G. Psakhie. Int. J. Adv. Manuf. Technol. 99, 2353 (2018). Crossref
10. A. Vorontsov, S. Astafurov, E. Melnikov, V. Moskvina, E. Kolubaev, E. Astafurova. Mater. Sci. Eng. A. 820, 141519 (2021). Crossref
11. N.N. Resnina, I.A. Palani, P.S. Liulchak, S.P. Belyaev, S.S. Mani Prabu, S. Jayachandran, V.D. Kalganov. Lett. Mater. 10 (4), 496 (2020). Crossref
12. S.D. Antolovich, R.W. Armstrong. Progress Mater. Sci. 59, 1 (2014). Crossref